

# Poisson Ratio of Epitaxial Germanium Films Grown on Silicon

JAYESH BHARATHAN,<sup>1,2,3</sup> JAGDISH NARAYAN,<sup>1</sup> GEORGE ROZGONYI,<sup>1</sup>  
and GARY E. BULMAN<sup>2</sup>

1.—Department of Materials Science and Engineering, North Carolina State University, Raleigh, NC 27695, USA. 2.—RTI International, Durham, NC 27709, USA. 3.—e-mail: jmbharat@ncsu.edu

An accurate knowledge of elastic constants of thin films is important in understanding the effect of strain on material properties. We have used residual thermal strain to measure the Poisson ratio of Ge films grown on Si  $\langle 001 \rangle$  substrates, using the  $\sin^2\psi$  method and high-resolution x-ray diffraction. The Poisson ratio of the Ge films was measured to be 0.25, compared with the bulk value of 0.27. Our study indicates that use of Poisson ratio instead of bulk compliance values yields a more accurate description of the state of in-plane strain present in the film.

**Key words:** Germanium film, Poisson ratio, x-ray diffraction

The presence of residual strain can have a significant effect on material properties of thin films. In the case of epitaxial germanium (Ge) thin films grown on silicon (Si), the presence of residual in-plane tensile strain leads to a decrease in its direct as well as indirect band gap.<sup>1,2</sup> Residual strain in thin films consists of three components: (i) lattice misfit strain, (ii) thermal misfit strain (coefficient of thermal expansion, CTE), and (iii) defect strain.<sup>3</sup> The lattice misfit strain is given by  $[1 - (a_{\text{Ge}}/a_{\text{Si}})]$ , where  $a_{\text{Ge}}$  (0.56 nm) and  $a_{\text{Si}}$  (0.54 nm) are the lattice parameters of Ge and Si, respectively. This translates to an in-plane misfit strain of  $-4.2\%$ . The negative sign indicates compressive strain in the Ge film. Since the critical thickness for pseudomorphic epitaxial growth of Ge on Si is  $\sim 1$  nm,<sup>4</sup> the misfit component is expected to be fully relaxed for films grown at elevated temperatures via the formation of dislocations that nucleate at the free surface and glide to the interface.<sup>5</sup> On the other hand, the thermal component of the residual strain is proportional to  $(\Delta\alpha \times \Delta T)$ , where  $\Delta\alpha$  is the difference in coefficients of thermal expansion of Si and Ge in the temperature interval  $\Delta T$ . This strain is expected to be on the order of  $+0.24\%$ , where the positive sign indicates tensile strain in the film. The magnitude of the thermal strain is much smaller and also opposite in sign

compared with the misfit strain. The thermal strain is expected to be unrelaxed since the mechanism of relaxation involves the nucleation of dislocations and glide in a relatively thick film. The residual strain in Ge has been experimentally shown to be tensile, and the thermal misfit component was conjectured to be one of two possible causes of this residual strain.<sup>2</sup> Since elastic constants of Ge thin films are not experimentally known, the in-plane strain is normally calculated using bulk elastic compliances of Ge and experimentally measured perpendicular strain using x-ray diffraction. The drawback of this approach is the implicit assumption that the elastic properties of thin films are the same as their bulk counterparts. The main purpose of this paper is to determine the Poisson ratio of Ge thin films using the high-resolution x-ray diffraction (HRXRD)<sup>6</sup> technique. Since the film has an inherent residual thermal strain, the principal idea is to measure the in-plane and parallel strain components in the film to compute the Poisson's ratio. Since the residual thermal strain is small, the measured strain should be related to the elastic response of the film rather than any plastic yield or inelastic phenomenon. A similar concept, which employed the use of a known residual thermal strain to measure yield stress by HRXRD, has been reported earlier for polycrystalline Pb<sup>7</sup> and Al-2%Cu<sup>8</sup> thin films on Si.

Epitaxial Ge films with two-dimensional morphology were grown on  $\langle 001 \rangle$  Si substrates by the commonly used two-step growth technique.<sup>9</sup> The

(Received August 15, 2012; accepted October 26, 2012;  
published online November 10, 2012)

range of misorientation of the  $\langle 001 \rangle$  Si substrates used for growth was  $\pm 0.5^\circ$ . Growth was carried out in a reduced-pressure chemical vapor deposition (RPCVD) system at pressure of 40 Torr using 1%  $\text{GeH}_4$ . A  $\sim 50$ -nm-thick Ge buffer layer was grown at  $360^\circ\text{C}$ , followed by thick Ge growth at  $700^\circ\text{C}$ . Three films of thicknesses  $0.7\ \mu\text{m}$  (sample A),  $1.7\ \mu\text{m}$  (sample B), and  $3.5\ \mu\text{m}$  (sample C) were grown for this study (Table I). The samples were annealed *in situ* at  $900^\circ\text{C}$  for 1 h to reduce the density of threading dislocations (TDs).<sup>10</sup> The counterparts to samples A and B, grown without *in situ* annealing, were also included for comparison. The motivation behind this selection was to study the sensitivity of the measured Poisson ratio to the defect density and film thickness. Residual strain was measured by HRXRD using a PANalytical X'Pert XRD system. The incident beam optics included a symmetrical  $4\times$  Ge  $\langle 220 \rangle$  crystal coupled with a divergence slit of  $0.5\ \text{mm}$ , and the diffracted beam optics included a  $1\text{-mm}$  slit placed in front of the detector. The  $2\theta$  step size used in the  $2\theta$ - $\omega$  scan was  $0.001^\circ$ . Cross-sectional transmission electron microscopy (TEM) was performed on a Hitachi HF 2000 microscope operated at 200 kV. Scanning electron microscopy (SEM) images were acquired using a Hitachi S800 microscope. Lastly, tapping-mode atomic force microscopy (AFM) images were obtained using a Digital Instrument 3100 scanning probe microscope.

Stress ( $\sigma$ ) and strain ( $\varepsilon$ ) in a three-dimensional isotropic system, in biaxial strain, are related by the following basic equations:<sup>11</sup>

$$\varepsilon_{11} = \frac{1}{E} [\sigma_{11} - \nu(\sigma_{22} + \sigma_{33})], \quad (1)$$

$$\varepsilon_{22} = \frac{1}{E} [\sigma_{22} - \nu(\sigma_{11} + \sigma_{33})], \quad (2)$$

$$\varepsilon_{33} = \frac{1}{E} [\sigma_{33} - \nu(\sigma_{11} + \sigma_{22})], \quad (3)$$

where  $\nu$  is the Poisson ratio of the material, an elastic constant that is the ratio of the lateral and axial strain, and  $E$  is the Young's modulus. Since residual stress exists only within the plane of the epitaxial film but not in the  $z$  direction,  $\sigma_{33} = 0$ . The above expressions can be rewritten as

$$\varepsilon_{11} + \varepsilon_{22} = \frac{1 - \nu}{E} [\sigma_{11} + \sigma_{22}], \quad (4)$$

$$\varepsilon_{33} = \frac{-\nu}{(1 - \nu)} [\varepsilon_{11} + \varepsilon_{22}]. \quad (5)$$

Since  $\varepsilon_{11} = \varepsilon_{22}$  for isotropic biaxial strain, we have

$$\nu = \frac{\varepsilon_{33}}{\varepsilon_{33} - 2\varepsilon_{11}}. \quad (6)$$

Equation 6 describes the fundamental relationship between in-plane strain ( $\varepsilon_{11}$ ,  $\varepsilon_{22}$ ) and perpendicular strain ( $\varepsilon_{33}$ ) in terms of the Poisson ratio. Inspection of Eq. 6 shows that the Poisson ratio for epitaxial films under biaxial strain can be easily calculated if the in-plane strain is known. One method to determine in-plane strain using HRXRD is the  $\sin^2\psi$  technique.

The analysis of the residual strain using x-ray diffraction is based on the measurement of interplanar spacing in different macroscopic directions. In the case of a rotationally symmetrical biaxial state of the residual stress, the dependence of the elastic lattice deformation on the inclination from the perpendicular direction,  $\psi$ , can be expressed by the  $\sin^2\psi$  formula, which predicts a linear behavior of the lattice constant with  $\sin^2\psi$ .<sup>3,11</sup> Hence, if the lattice parameter is measured in several independent directions as a function of  $\psi$ , the extrapolated value of  $a_{\phi\psi}$  at  $\psi = 90^\circ$  yields the in-plane strain present in the film. Figure 1 shows a  $\langle 001 \rangle$  projection of a cubic crystal, with the dotted line in the figure representing planes that were used for strain measurements. Planes  $(004)$ ,  $(113)$ ,  $(115)$ ,  $(112)$ , and  $(111)$  in quadrant 1 (Q1) belong to zone axes  $[-110]$ , whereas planes  $(121)$  and  $(151)$  belong to the zone

**Table I. Characteristics of the Ge films grown on Si  $\langle 001 \rangle$  substrates for the determination of the Poisson ratio**

Sample	Thickness ( $\mu\text{m}$ )	Anneal	TDD ( $\text{cm}^{-2}$ )	RMS Roughness (nm)	$\varepsilon_{\perp}$	$\nu$	$R^2$
A	0.7	$900^\circ\text{C}$ , 1 h	$6.3 \pm 0.6 \times 10^6$	1.79	-0.122	0.252	0.9998
A*	0.7	NA	$1.1 \pm 0.8 \times 10^7$	1.09	-0.127	0.255	0.9909
B	1.7	$900^\circ\text{C}$ , 1 h	$1.4 \pm 0.5 \times 10^7$	1.09	-0.106	0.253	0.9925
B*	1.7	NA	$2.1 \pm 0.7 \times 10^8$	1.12	-0.118	0.250	0.9997
C	4.0	$900^\circ\text{C}$ , 1 h	$6.4 \pm 0.5 \times 10^6$	1.43	-0.103	0.249	0.9994

Samples without dislocation annealing are indicated with an asterisk. Threading dislocation densities (TDDs) were determined using etch pit density (EPD) analysis. Perpendicular strain ( $\varepsilon_{\perp}$ ) was measured using HRXRD, and Poisson ratio of Ge films was calculated using Eq. 6 (see text).

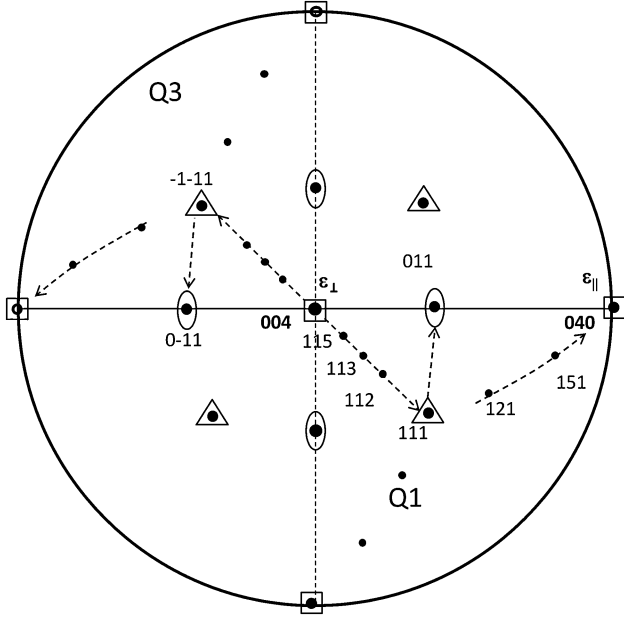


Fig. 1. Standard (001) stereographic projection of a cubic crystal. Dotted line shows the planes used to determine the lattice parameter in quadrant 1 (Q1) and quadrant 3 (Q3), respectively.

axes  $[-101]$ . Since the poles of planes other than (400) are inclined with respect to the perpendicular direction, appropriate  $\psi$  tilts were carried out to bring the pole of the plane parallel to the diffraction vector. The diffraction vector is the vector that bisects the angles of incidence and diffraction. Due to the tetragonal distortion present in Ge, the effect of tilt on strain measurements was corrected by taking two measurements for each  $(hkl)$ ,  $180^\circ$  apart in the  $\phi$  direction.<sup>12</sup> This is equivalent to two measurements made in the quadrants Q1 and Q3 for a given  $(hkl)$ . The average of the two measurements was used to calculate the lattice spacing,  $d_{hkl}$ , using Bragg's law.

The surface morphology of the Ge films was characterized using AFM (Fig. 2). All the films studied in this research exhibited root-mean-square (RMS) roughness of approximately 1 nm to 2 nm, which confirms the two-dimensional growth of the epitaxial Ge films and the existence of a uniform biaxial stress. The dark contrast seen in the unannealed samples (A\*, B\*) is quite likely pits corresponding to the surface termination of mixed dislocations.<sup>13</sup> The density of the pits is approximately  $6 \times 10^7 \text{ cm}^{-2}$  to  $8 \times 10^7 \text{ cm}^{-2}$ , which is consistent with values of threading dislocation densities (TDDs) found in literature for as-grown Ge film on Si.<sup>9</sup> The pits are not visible in the annealed samples, indicating a reduction in TDD by high-temperature annealing.

We confirmed these results by carrying out defect delineation studies on the films using a mixture of acetic acid (67 mL), nitric acid (20 mL), hydrofluoric

acid (10 mL), and iodine (30 mg). Figure 3 shows SEM micrographs of etched films that clearly show a drastic reduction in TDD on annealing; for example, the TDD in sample B decreases by almost an order of magnitude from  $2 \times 10^8 \text{ cm}^{-2}$  to  $1.0 \times 10^7 \text{ cm}^{-2}$  after annealing.

Figure 4 shows cross-sectional TEM micrographs of samples A and B\*. The TDD in sample B\* (unannealed  $1.7\text{-}\mu\text{m}$  Ge) was estimated to be  $1.28 \times 10^8 \text{ cm}^{-2}$ , i.e., very similar to the EPD and AFM analysis. The absence of threading segments in sample A (annealed  $0.7\text{-}\mu\text{m}$  Ge) signifies that the overall TDD in this film is less than  $2 \times 10^7 \text{ cm}^{-2}$ . It has been shown that TDs in Ge are of  $60^\circ$  glissile type, and the reduction in their density on annealing has been postulated to take place by thermal stress-induced glide and annihilation.<sup>14</sup>

The residual strain of all the films listed in Table I was characterized using HRXRD. Figure 5 shows the lattice parameter versus  $\sin^2\psi$  plot for sample A (annealed  $0.7\text{-}\mu\text{m}$  Ge) with data points fitted to a best-fit linear regression line along with the  $R^2$  value, a measure of the quality of fit. We obtained  $R^2$  values greater than 0.999, which confirms the linear relationship predicted by the  $\sin^2\psi$  method and also the high accuracy of the reported data. The in-plane lattice parameter was determined by extrapolation of the best-fit line to  $\sin^2\psi = 1$ . The calculated lattice parameters using different  $(hkl)$  as a function of  $\psi$  for sample A are listed in Table II.

The Poisson ratio in all the samples was found to be independent of film thickness as well as defect density (Table I). This is a further indication that the measured strain is associated with the elastic response of the film. The average of five measurements yielded a value of  $0.252 \pm 0.002$  for the Poisson ratio of Ge epitaxial films. The Poisson ratio of isotropic materials can be calculated from bulk elastic compliances using the expression  $\nu = C_{12}/(C_{11} + C_{12})$ , where  $C_{11}$  (129.2 GPa) and  $C_{12}$  (47.9 GPa) are the elastic compliances of bulk Ge at 300 K.<sup>15</sup> This gives a value of  $\nu = 0.27$  for Ge. This study shows that the Poisson ratio of Ge thin films is approximately 7% lower than that of bulk Ge.

The presence of impurities can be expected to affect the elastic properties of thin-film materials. It has been previously shown that the elastic constants in Ge are sensitive to the presence of dopants. Addition of 0.05% impurity resulted in a change of 5.5% in the elastic constant,  $C_{44}$ .<sup>16</sup> Secondary-ion mass spectrometry (SIMS) analysis of sample C ( $4.0\text{-}\mu\text{m}$  annealed Ge) was carried out to ascertain the purity of the Ge film (Fig. 6). The elements analyzed included carbon, oxygen, nitrogen, silicon, and boron (B). Carbon and oxygen are typical impurities that are present due to the relatively higher operating pressure used in RPCVD epitaxy, whereas boron was the dopant in the  $p$ -type Si substrates used for epitaxy. The analysis indicates

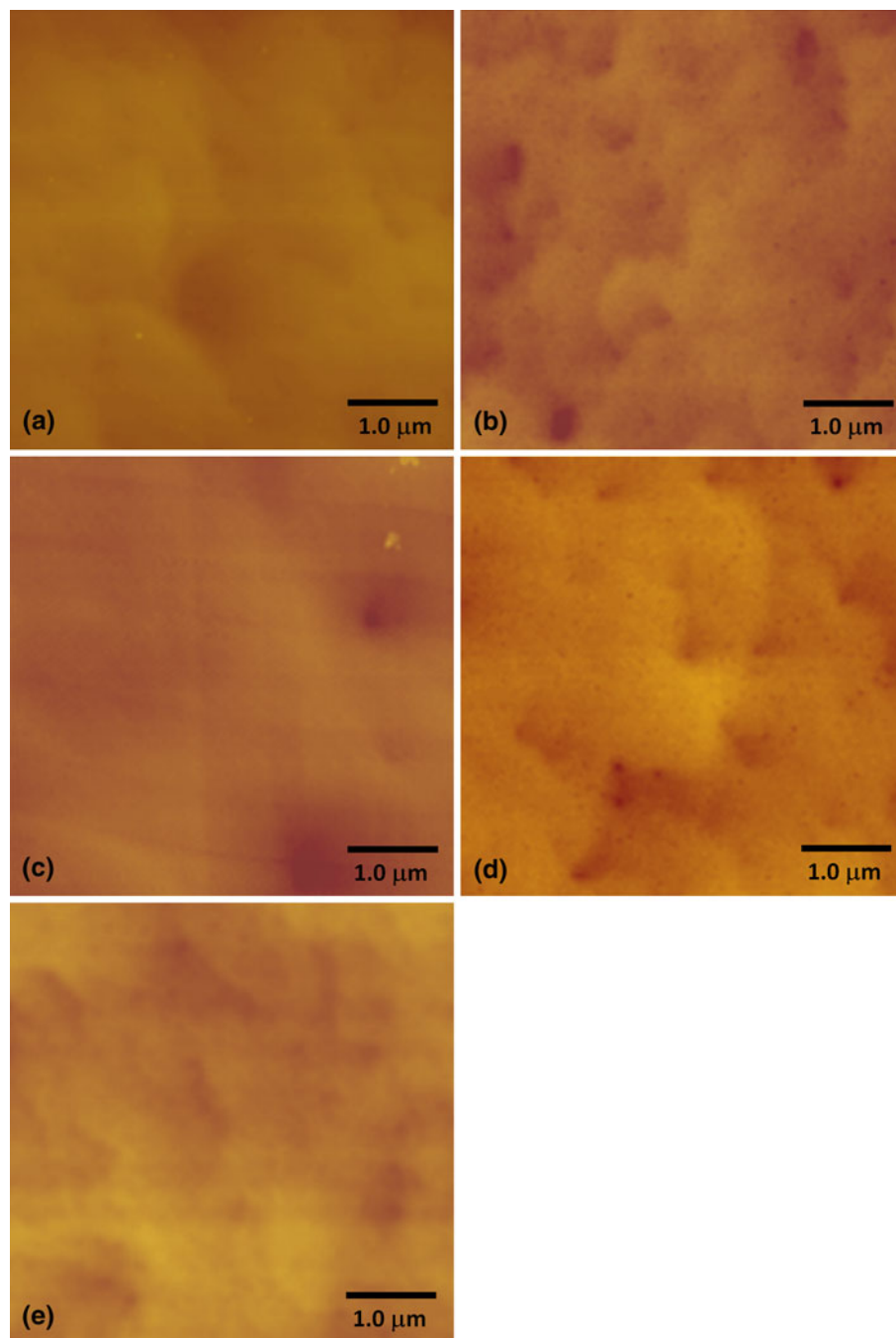


Fig. 2. Tapping-mode AFM images ( $5\ \mu\text{m} \times 5\ \mu\text{m}$ ) of the surface of (a) sample A, annealed  $0.7\text{-}\mu\text{m}$ -thick Ge film with RMS roughness of  $1.79\ \text{nm}$ , (b) sample A\*, unannealed  $0.7\text{-}\mu\text{m}$ -thick Ge film with RMS roughness of  $1.09\ \text{nm}$ , (c) sample B, annealed  $1.7\text{-}\mu\text{m}$ -thick Ge film with RMS roughness of  $1.09\ \text{nm}$ , (d) sample B\*, unannealed  $1.7\text{-}\mu\text{m}$ -thick Ge film with RMS roughness of  $1.12\ \text{nm}$ , (e) sample C, annealed  $4.0\text{-}\mu\text{m}$ -thick Ge film with RMS roughness of  $1.43\ \text{nm}$ .

some outdiffusion of Si atoms from the substrate into the Ge film. However, the concentration of all the elements studied was below the SIMS detection limit in the bulk of the Ge film. The diffusion of these elements can be expected to be substantially lower for samples that did not receive *in situ* dislocation annealing. This analysis shows that

impurities in the film have a negligible impact on the measured Poisson ratio.

Lastly, the impact of using the bulk Poisson ratio in strain calculations is considered. The average perpendicular strain measured in the Ge epitaxial films was  $-0.114\%$ . The calculated in-plane strain using Eq. 5 and Poisson ratio of  $0.25$  and  $0.27$  is



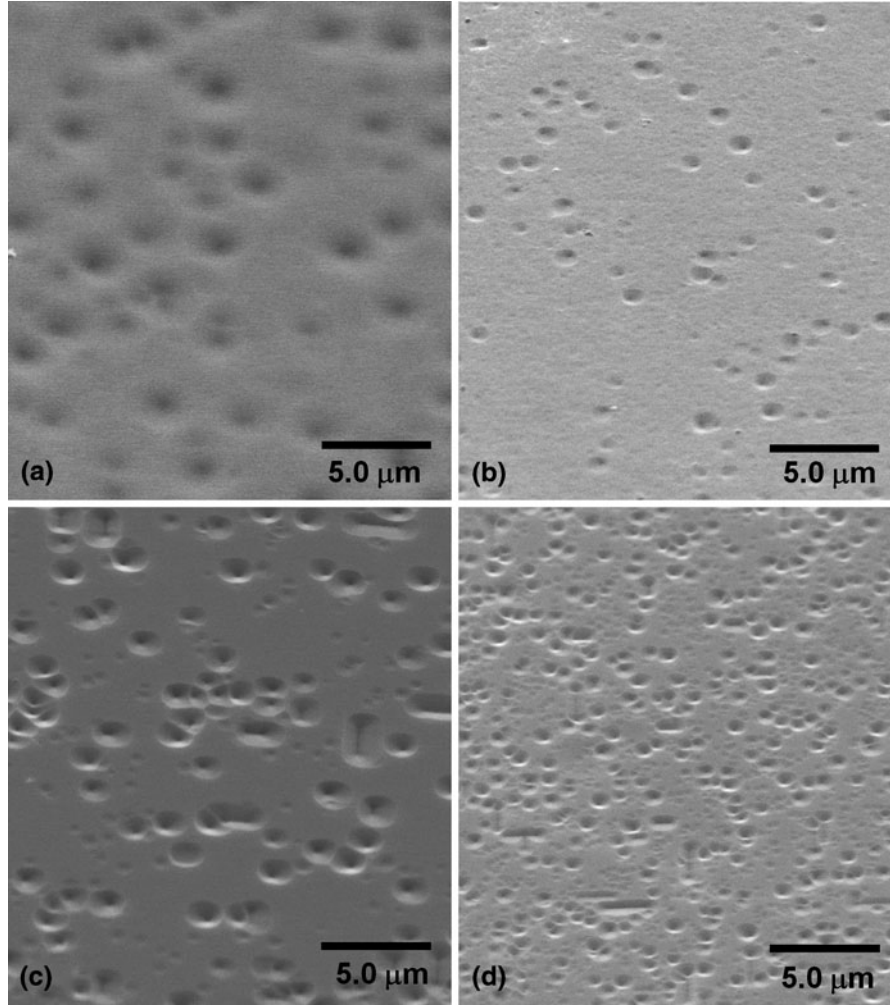


Fig. 3. EPD results showing TDD in the various films: (a) sample A, annealed 0.7- $\mu\text{m}$ -thick Ge film with EPD of  $6.3 \times 10^6 \text{ cm}^{-2}$ ; (b) sample A\*, unannealed 0.7- $\mu\text{m}$ -thick Ge film with EPD of  $1.1 \times 10^7 \text{ cm}^{-2}$ ; (c) sample B, annealed 1.7- $\mu\text{m}$ -thick Ge film with EPD of  $1.1 \times 10^7 \text{ cm}^{-2}$ ; (d) sample B\*, unannealed 1.7- $\mu\text{m}$ -thick Ge film with EPD of  $2.0 \times 10^8 \text{ cm}^{-2}$ .

+0.183% and +0.162%, respectively, which yields a difference of 0.02%. Since growth was carried out at 700°C, the theoretically expected thermal misfit strain on cooling to room temperature is +0.24%, which was calculated using

$$\varepsilon_{||} = \int_{T_{\text{RT}}}^{T_{\text{GR}}} [\alpha_{\text{Ge}}(T) - \alpha_{\text{Si}}(T)] dT, \quad (7)$$

where  $T_{\text{RT}}$  and  $T_{\text{GR}}$  are the room temperature and growth temperature, respectively, and  $\alpha_{\text{Ge}}$  and  $\alpha_{\text{Si}}$  are the thermal expansion coefficients of Ge and Si.<sup>17,18</sup> Although the magnitude of the residual strain is small, it has a tremendous impact on the optoelectronic properties of epitaxial Ge. It has been shown that in-plane tensile strain on the order of +0.18% decreases the direct band gap of Ge by approximately

20 meV, which corresponds to a 30 nm shift of the band edge.<sup>19</sup> Hence, precise knowledge of the Poisson ratio is essential in studying the impact of strain on the optoelectronic properties of thin films. Clearly, use of bulk elastic constants results in appreciable error in the strain calculation of thin films.

In conclusion, we have measured the Poisson ratio of epitaxial Ge films on Si using HRXRD. Our measurements indicate that the Poisson ratio of epitaxial Ge films is lower (0.25) than bulk Ge (0.27). The use of a thin-film elastic constant gives a more accurate description of the residual strain present in the epitaxial film.

This work made use of the HRXRD system at the Shared Materials Instrumentation Facility at Duke University. The authors would like to thank Dr. Mark Walters at Duke University for his help with the XRD system, and Dr. Rama Venkatasubramanian,

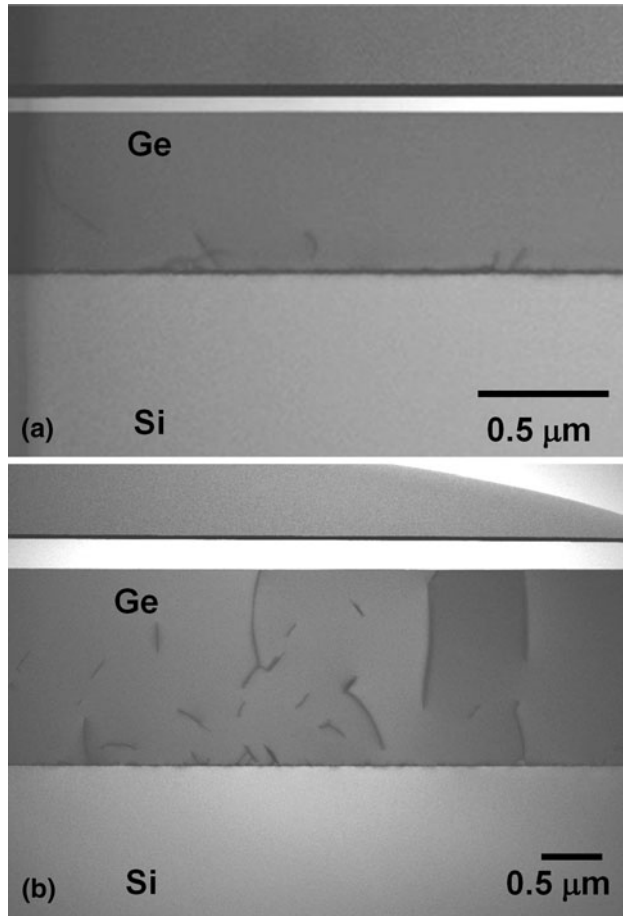


Fig. 4. Cross-sectional bright-field TEM images of (a) sample A, annealed 0.7- $\mu\text{m}$ -thick Ge film, (b) sample B\* unannealed 1.7- $\mu\text{m}$ -thick Ge film with EPD of  $2.0 \times 10^8 \text{ cm}^{-2}$ . The dark contrast in sample B\* corresponds to threading dislocation segments that terminate at the surface of the film.

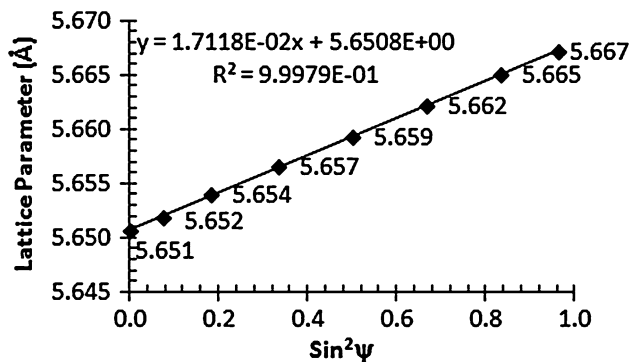


Fig. 5. Lattice parameter as a function of  $\sin^2 \psi$  ( $\psi$  is the angle of the diffraction plane normal away from the surface normal) for sample A (0.7  $\mu\text{m}$  annealed Ge).

Dr. Philip Barletta, and Jonathan Pierce from RTI International for their valuable feedback. The work was supported by RTI International.

Table II. Measured lattice parameter for sample A (0.7  $\mu\text{m}$  annealed Ge) as a function of  $\psi$

(hkl)	$\psi$ ( $^\circ$ )	$a$ (nm)
(400)	0	5.651
(113), (-1-13)	15.8	5.652
(112), (-1-12)	25.2	5.654
(011), (0-11)	35.3	5.657
(111), (-111)	45	5.659
(044), (0-44)	54.8	5.662
(121), (-1-21)	65.9	5.665
(151), (-1-51)	78.9	5.667

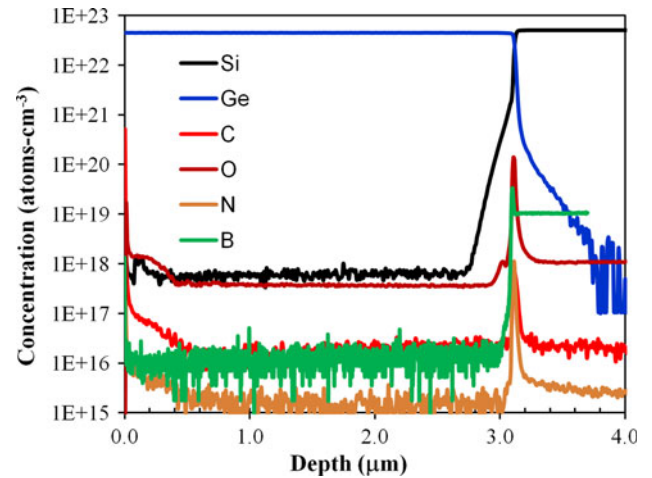


Fig. 6. SIMS profiling of carbon, oxygen, nitrogen, silicon, and boron in sample C (4.0  $\mu\text{m}$  annealed Ge).

## REFERENCES

1. C.G. Van de Walle, *Phys. Rev. B* 39, 1871 (1989).
2. D.D. Cannon, J. Liu, Y. Ishikawa, K. Wada, D.T. Danielson, S. Jongthammanurak, J. Michel, and L.C. Kimerling, *Appl. Phys. Lett.* 84, 906 (2004).
3. P. Pant, J.D. Budai, and J. Narayan, *Acta Mater.* 58, 1097 (2010).
4. D.J. Eaglesham and M. Cerullo, *Phys. Rev. Lett.* 64, 1943 (1990).
5. S. Oktyabrsky and J. Narayan, *Philos. Mag. A* 72, 305 (1995).
6. G. Cornella, S.-H. Lee, W.D. Nix, and J.C. Bravman, *Appl. Phys. Lett.* 71, 2949 (1997).
7. T.S. Kuan and M. Murakami, *Metall. Trans. A* 13A, 383 (1982).
8. C.J. Shute and J.B. Cohen, *J. Mater. Res.* 6, 950 (1991).
9. J. Michel, J. Liu, and L.C. Kimerling, *Nat. Photonics* 4, 527 (2010).
10. L. Colace, G. Masini, G. Assanto, H.-C. Luan, K. Wada, and L.C. Kimerling, *Appl. Phys. Lett.* 76, 1231 (2000).
11. I.C. Noyan and J.B. Cohen, *Residual Stress Measurement by Diffraction and Measurement* (New York: Springer, 1987).
12. D.K. Bowen and B.K. Tanner, *High Resolution X-ray Diffractometry and Topography* (Bristol: Taylor & Francis, 2005), p. 60.
13. P. Visconti, K.M. Jones, M.A. Reshchikov, R. Cingolani, H. Morkoc, and R.J. Molnar, *Appl. Phys. Lett.* 77, 3532 (2000).
14. H.C. Luan, R.L. Desmond, K.K. Lee, K.M. Chen, J.G. Sandland, K. Wada, and L.C. Kimerling, *Appl. Phys. Lett.* 75, 2909 (1999).

15. J.J. Wortman and R.A. Evans, *J. Appl. Phys.* 36, 153 (1965).
16. L.J. Bruner and R.W. Keyes, *Phys. Rev. Lett.* 7, 55 (1961).
17. H.P. Singh, *Acta Crystallogr. A* 24, 469 (1968).
18. Y. Okada and Y. Tokamaru, *J. Appl. Phys.* 56, 314 (1984).
19. J.M. Hartmann, A. Abbadie, A.M. Papon, P. Holliger, G. Rolland, T. Billon, M. Rouviere, L. Vivien, and S. Laval, *J. Appl. Phys.* 95, 5905 (2004).